

# Nonergodicity and Central Limit Behavior for Long-range Hamiltonians

A. PLUCHINO<sup>1</sup>, A. RAPISARDA<sup>1</sup> and C. TSALLIS<sup>2,3</sup>

<sup>1</sup> *Dipartimento di Fisica e Astronomia, Università di Catania, and INFN sezione di Catania, - Via S. Sofia 64, I-95123 Catania, Italy*

<sup>2</sup> *Centro Brasileiro de Pesquisas Físicas, - Rua Xavier Sigaud 150, 22290-180 Rio de Janeiro-RJ, Brazil*

<sup>3</sup> *Santa Fe Institute, 1399 Hyde Park Road, Santa Fe, NM 87501, USA*

PACS 64.60.My – Metastable phases

PACS 89.75.-k – Complex systems

**Abstract.** – We present a molecular dynamics test of the Central Limit Theorem (CLT) in a paradigmatic long-range-interacting many-body classical Hamiltonian system, the HMF model. We calculate sums of velocities at equidistant times along deterministic trajectories for different sizes and energy densities. We show that, when the system is in a chaotic regime (specifically, at thermal equilibrium), ergodicity is essentially verified, and the Pdfs of the sums appear to be Gaussians, consistently with the standard CLT. When the system is, instead, only weakly chaotic (specifically, along longstanding metastable Quasi-Stationary States), nonergodicity (i.e., discrepant ensemble and time averages) is observed, and robust  $q$ -Gaussian attractors emerge, consistently with recently proved generalizations of the CLT.

**Introduction.** – During recent years there has been an increasing interest in generalizations of the Central Limit Theorem (CLT). This theorem – so called because of its central position in theory of probabilities – has ubiquitous and important applications in several fields. It essentially states that a (conveniently scaled) sum of  $n \rightarrow \infty$  independent (or nearly independent) random variables with finite variance has a Gaussian distribution. Understanding, this theorem is not applicable to those complex systems where long-range correlations are the rule, such as those addressed by nonextensive statistical mechanics [1, 2]. Therefore, several papers [3–10] have recently discussed extensions of the CLT and their corresponding attractors. In this paper, following [5, 6], we present several numerical simulations for a long-range Hamiltonian system, namely the Hamiltonian Mean Field (HMF) model. This model is a paradigmatic one for classical Hamiltonian systems with long-range interactions which has been intensively studied in the last decade (see, for example, [6, 12–22], and references therein). In [5] it was shown that the probability density of rescaled sums of iterates of deterministic dynamical systems (e.g., the logistic map) at the edge of chaos (where the Lyapunov exponent vanishes) violates the CLT. Here we study rescaled sums of velocities considered along deterministic trajectories in the

HMF model. It is well known that, in this model, a wide class of out-of-equilibrium initial conditions induce a violent relaxation followed by a metastable regime characterized by nearly vanishing (strictly vanishing in the thermodynamic limit) Lyapunov exponents, and glassy dynamics [15–17]. We exhibit that correlations and nonergodicity created along these Quasi-Stationary States (QSS) can be so strong that, when summing the velocities calculated during the deterministic trajectories of single rotors at fixed intervals of time, the standard CLT is no longer applicable. In fact, along the QSS,  $q$ -Gaussian Pdfs emerge as attractors instead of simple Gaussian Pdfs, consistently with the recently advanced  $q$ -generalized CLT [4, 5, 9], and ensemble averages are different from time averages.

**Numerical simulations.** – The HMF model describes a system of  $N$  fully-coupled classical inertial XY spins (rotors)  $\vec{s}_i = (\cos \theta_i, \sin \theta_i)$ ,  $i = 1, \dots, N$ , with unitary module and mass [12, 13]. These spins can also be thought as particles rotating on the unit circle. The Hamiltonian is given by

$$H = \sum_{i=1}^N \frac{p_i^2}{2} + \frac{1}{2N} \sum_{i,j=1}^N [1 - \cos(\theta_i - \theta_j)] , \quad (1)$$

where  $\theta_i$  ( $0 < \theta_i \leq 2\pi$ ) is the angle and  $p_i$  the conjugate variable representing the rotational velocity of spin  $i$ .

The equilibrium solution of the model in the canonical ensemble predicts a second order phase transition from a high temperature paramagnetic phase to a low temperature ferromagnetic one [12]. The critical temperature is  $T_c = 0.5$  and corresponds to a critical energy per particle  $U_c = E_c/N = 0.75$ . The order parameter of this phase transition is the modulus of the *average magnetization* per

spin defined as:  $M = (1/N) |\sum_{i=1}^N \vec{s}_i|$ . Above  $T_c$ , the spins point in different directions and  $M \sim 0$ . Below  $T_c$ , most spins are aligned (the rotators are trapped in a single cluster) and  $M \neq 0$ . The out-of-equilibrium dynamics of the model is also very interesting. In a range of energy densities between  $U \in [0.5, 0.75]$ , special initial conditions called *water-bag* (characterized by initial magnetization  $M_0 = 1$  and uniform distribution of the momenta) drive the system, after a violent relaxation, towards metastable QSS. The latter slowly decay towards equilibrium with a lifetime which diverges like a power of the system size  $N$  [14–16].

In this section we simulate the dynamical evolution of several HMF systems with different sizes and at different energy densities, in order to explore their behavior either inside or outside the QSS regime. For each of them, following the prescription of the CLT, we construct probability density functions of quantities expressed as a finite sum of stochastic variables. But in this case, following the procedure adopted in ref. [5] for the logistic map, we will select these variables along the deterministic time evolutions of the  $N$  rotors. More formally, we study the Pdf of the quantity  $y$  defined as

$$y_j = \frac{1}{\sqrt{n}} \sum_{i=1}^n (p_j(i) - \langle p_j \rangle) \quad \text{for } j = 1, 2, \dots, N, \quad (2)$$

where  $p_j(i)$ , with  $i = 1, 2, \dots, n$ , are the velocities of the  $j$ th-rotor taken at fixed intervals of time  $\delta$  along the same trajectory. The latter are obtained integrating the HMF equations of motions (see [15] for details about these equations and the integration algorithm adopted). The quantity  $\langle p_j \rangle = (1/n) \sum_{i=1}^n p_j(i)$  is the average of the  $p_j(i)$ 's over the single trajectory. The product  $\delta \times n$  gives the total simulation time. Note that the variables  $y$ 's are proportional to the *time average* of the velocities along the single rotor trajectories. In the following we will distinguish this kind of average, i.e. *time average*, from the standard *ensemble average*, where the average of the velocities of the  $N$  rotators is calculated at a *given fixed time* and over many different realizations of the dynamics. The latter can also be obtained from eq.(2) considering the  $y$ 's variables with  $n = 1$  and  $\langle p_j \rangle = 0$ . In general, although the standard CLT predicts a Gaussian shape for sum of  $n$  independent stochastic values strictly when  $n \rightarrow \infty$ , in practice a finite sum converges quite soon to the Gaussian shape and this, in absence of correlations, is certainly true

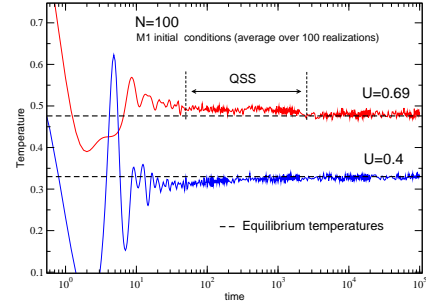


Fig. 1: Temperature time evolution for the HMF system, with  $N=100$  and M1 initial conditions, for  $U = 0.69$  and for  $U = 0.4$ . The presence of a QSS regime is visible only in the  $U = 0.69$  case, although a transient regime exist also for  $U = 0.4$ .

at least for the central part of the distribution [24]. Typically we will use in this section a sum of  $n = 50$  values of velocities along the deterministic trajectories for each of the  $N$  rotors of the HMF system, though larger values of  $n$  were also considered.

In the following we will show that, if correlations among velocities are strong enough and the system is weakly chaotic, CLT predictions are not verified and, consistently with recent generalizations of the CLT,  $q$ -Gaussians appear [3–5]. The latter are a generalization of Gaussians which emerge in the context of nonextensive statistical mechanics [1, 2] and are defined as

$$G_q(x) = A(1 - (1 - q)\beta x^2)^{1/(1-q)}, \quad (3)$$

being  $q$  the so-called *entropic index* (for  $q = 1$  one recovers the usual Gaussian),  $\beta$  another suitable parameter (characterizing the width of the distribution), and  $A$  a normalization constant (see also ref. [10] for a simple and general way to generate them). In particular we will show in this section that:

(i) *at equilibrium*, when correlations are weak and the system is strongly chaotic (hence ergodic) standard CLT is verified, and time average coincides with ensemble average (both corresponding Pdfs are Gaussians, either in the limit  $n \rightarrow \infty$  or  $\delta \rightarrow \infty$ );

(ii) *in the QSS regime*, where velocities are strongly correlated and the system is weakly chaotic and nonergodic, the standard CLT is no longer applicable, and  $q$ -Gaussian attractors replace the Gaussian ones; in this regime ensemble averages do not agree with time averages.

For all the present simulations, water-bag initial conditions with initial magnetization  $M_0 = 1$ , usually referred as M1, will be used. In general, several different realizations of the initial conditions will be performed also for the time average Pdfs case, but only in order to have a good statistics for small values of  $N$  (for  $N=50000$ , on the contrary, only one realization has been used: see fig.7(b)). Finally, to allow a correct comparison with standard Gaussians (represented as dashed lines in all the figures) and  $q$ -Gaussians (represented as full lines), the Pdf curves were

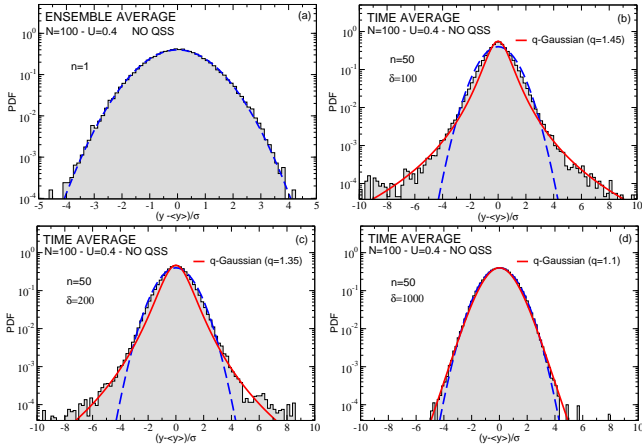


Fig. 2: Numerical simulations for the HMF model with  $N=100$ ,  $U=0.4$  and M1 initial conditions. No QSS are present for this energy value. (a) We plot here the Pdf of the single rotor velocities at the time  $t=40000$  (ensemble average over 1000 realizations), i.e. we plot the (normalized) variable  $y$  defined as in eq.(2) with  $n=1$ . The shape is Gaussian since the system is at equilibrium. In the other figures (b), (c) and (d) we plot the time average Pdfs for the normalized variable  $y$ , with  $n=50$  but with different time intervals ( $\delta=100, 200$  and  $1000$ ), calculated over an increasing simulation time after a transient of 40000 time units. An average over 1000 different realizations of the initial conditions was also considered in order to have a good statistics. Even if we are at equilibrium, it is evident a strong dependence of the entropic index  $q$  of the  $q$ -Gaussian fitting curve on the time interval  $\delta$  adopted. Anyway, a time interval  $\delta=1000$  is already sufficient to obtain a Gaussian-shaped Pdf. See text for further details.

always normalized to unit area and unit variance, by subtracting from the  $y$ 's their average  $\langle y \rangle$  and dividing by the correspondent standard deviation  $\sigma$  (hence, the traditional  $\sqrt{n}$  scaling adopted in Eq. (2) is in fact irrelevant).

*The case  $N=100$ .* We start the discussion of the numerical simulations for the HMF model considering a size  $N=100$  and two different energy densities,  $U=0.4$  and  $U=0.69$ . In the first case no QSS exist, while in the second case QSS characterize the out-of-equilibrium dynamics and correlations formed during the first part of the dynamics decay slowly while the system relaxes towards equilibrium [15, 16]. With  $N=100$  this relaxation takes however a reasonable amount of time steps, thus one can easily study also the equilibrium regime. The situation is illustrated in fig. 1, where we show the time evolution of the temperature - calculated as twice the average kinetic energy per particle - for the two energy densities considered, starting from  $M_0=1$  initial conditions. As expected QSS are clearly visible only in the case  $U=0.69$ , although a small transient regime exists also for the case  $U=0.4$  [15].

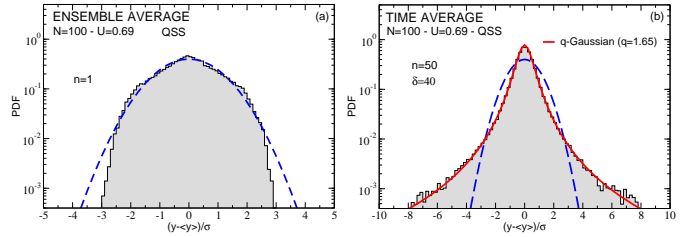


Fig. 3: Numerical simulations for the HMF model, with  $N=100$  and  $U=0.69$  and M1 initial conditions. We are in this case *inside the QSS regime*. (a) We plot here the Pdf of the single rotor velocities at time  $t=100$  (ensemble average over 1000 realizations). The shape is not Gaussian. (b) Time average Pdf for the normalized variable  $y$  with  $n=50$  and with a time interval  $\delta=40$ , calculated after a transient time of 100 time units. An average over 1000 different realizations of the initial conditions was also considered in order to have a good statistics. The resulting shape is very different from that one shown in (a) and can be very well fitted with a  $q$ -Gaussian.

*$N=100$  and  $U=0.4$ .* Here we discuss numerical simulations for the HMF model with size  $N=100$  and  $U=0.4$ . In this case it has been shown in the past that the equilibrium regime is reached quite fast and is characterized by a very chaotic dynamics [12, 13].

In fig. 2 a transient time of 40000 units has been performed before the calculations, so that the equilibrium is fully reached (see fig.1). In (a) we consider the ensemble average of the velocities, i.e. the  $y$  variables defined as in (2) with  $n=1$ , at  $t=40000$  and taking 1000 different realizations of the initial conditions (events). The Pdf compares very well with the Gaussian curve (dashed line), as expected at equilibrium. On the other hand, we consider in (b), (c) and (d) the Pdfs for the variable  $y$  with  $n=50$  and with different time intervals  $\delta$  over an increasing simulation time at equilibrium. As previously explained, this procedure corresponds to performing a time average along the trajectory for all the rotors of the system. In this case only the central part of the curve exhibits a Gaussian shape. On the other hand, Pdfs have long fat tails which can be very well reproduced with  $q$ -Gaussians (full lines). If one increases the time interval  $\delta$  going from  $\delta=100$  (b), to  $\delta=200$  (c) and finally to  $\delta=1000$  (d), the tails tend to disappear, the entropic index  $q$  of the  $q$ -Gaussians decreases from  $q=1.45 \pm 0.05$  towards  $q=1$  and the Pdf tends to the standard Gaussian. This means that, as expected, summed velocities are less and less correlated as  $\delta$  increases (see also ref. [5]) and therefore the assumptions of the CLT are satisfied as well as its prediction. Notice that  $n=50$  terms and a time interval  $\delta=1000$  are sufficiently large to reach a Gaussian-shaped Pdf. This situation reminds similar observations in the analysis of returns in financial markets [24], or in turbulence [25].

*$N=100$  and  $U=0.69$ .* Let us to consider now numerical simulations for the HMF model with size  $N=100$  and

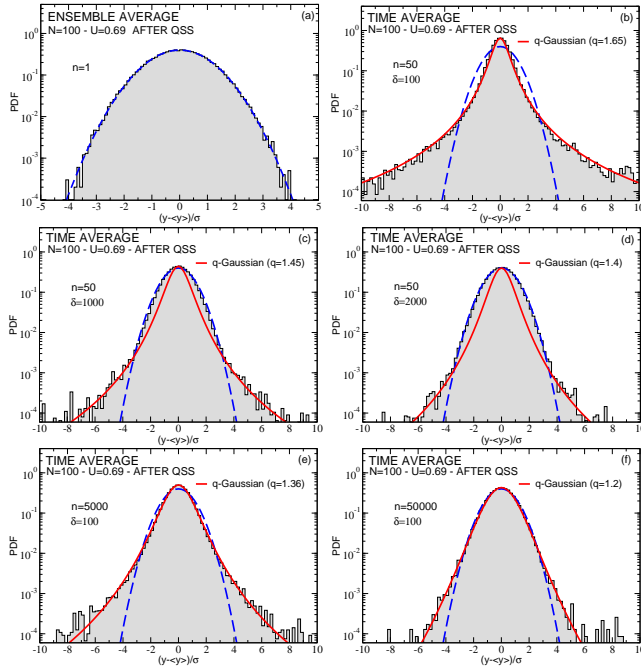


Fig. 4: Numerical simulations for the HMF model, with  $N = 100$ ,  $U = 0.69$  and M1 initial conditions. We are here *after the QSS regime*. (a) Pdf of the single rotor velocities at  $t=40000$  (ensemble average over 1000 realizations). The shape is Gaussian since the system is at equilibrium. In the other figures we plot the time average Pdfs for the normalized variable  $y$ , calculated after a transient time of 40000. An average over 1000 different realizations of the initial conditions was also considered in order to have a good statistics. In figs.(b-d) we considered  $n = 50$  but with different time intervals, more precisely  $\delta=100$  (b),  $\delta=1000$  (c) and  $\delta=2000$  (d), over an increasing simulation time at equilibrium. (e)-(f) Pdfs obtained by keeping fixed the value  $\delta = 100$  and increasing the number  $n$  of velocities in the sum for getting  $y$ . More precisely,  $n = 5000$  in (e) and  $n = 50000$  in (f). It is clear that, both for  $\delta \rightarrow \infty$  and  $n \rightarrow \infty$ , the Pdfs shape tends to a Gaussian.

$U = 0.69$ . In this case a QSS regime exists, but its characteristic lifetime is quite short since the noise induced by the finite size drives the system towards equilibration rapidly. However strong correlations, created by the M1 initial conditions, exist and their decay is slower than in the case  $U = 0.4$ . In fig. 3 we show in (a) the Pdf of the velocities calculated at  $t = 100$  (i.e. at the beginning of the QSS regime). An ensemble average over 1000 realizations was considered. The Pdf shows a strange shape which remains constant in the QSS, as already observed in the past [14], and which differs from both the Gaussian and the  $q$ -Gaussian curves. On the other hand, we show in (b) the Pdf of the variable  $y$  with  $n = 50$  and  $\delta = 40$ , i.e. calculated over a total of 2000 time steps after a transient of 100 units, in order to stay inside the QSS temperature plateaux (see fig.1). In this case the system is weakly chaotic and non ergodic [15, 16] and the numerical Pdf is reproduced very well by a  $q$ -Gaussian with  $q = 1.65 \pm 0.05$ .

Although in this case we have used different initial conditions also for time averages, these results provide a first indication that ensemble and time averages are inequivalent in the QSS regime. Note that, due to the shortness of the QSS plateaux, for  $N = 100$  it is not possible to use greater values of  $\delta$  or  $n$  in the numerical calculations of the  $y$ 's.

In fig.4 we repeat the previous simulations for  $N = 100$  and  $U = 0.69$ , but adopting a transient time of 40000 steps, in order to study the behavior of the system *after* the QSS regime. The ensemble average Pdf (over 1000 realizations) of the single rotor velocities at the time  $t = 40000$  is shown in (a) and indicates that equilibrium seems to have been reached. In fact the agreement with the standard Gaussian is almost perfect up to  $10^{-4}$ . In the other figures we plot the time average Pdfs for the variable  $y$  with  $n = 50$  and for different time intervals  $\delta$ , as done for  $U = 0.4$ . More precisely  $\delta=100$  in (b),  $\delta=1000$  in (c) and  $\delta=2000$  in (d). Again it is evident a strong dependence of the Pdf shapes on the time interval  $\delta$  adopted. In fact initially (b) the Pdf is well fitted by a  $q$ -Gaussian with a  $q = 1.65 \pm 0.05$ , however increasing  $\delta$ , in (c) and (d), the central part of the Pdf becomes Gaussian while tails are still present and can be well fitted by  $q$ -Gaussians with values of  $q$  that tend towards unity. However, at variance with the  $U = 0.4$  case, in this case not even a time interval  $\delta = 2000$  is sufficient to reach a complete Gaussian-shaped Pdf down to  $10^{-4}$ : evidently the strong correlations characterizing the QSS regime decay very slowly even after it, making the equilibrium shown by the ensemble average Pdf in (a) only apparent. This means that full ergodicity, i.e., full equivalence between ensemble and time averages, is reached, in this case, only asymptotically.

The last statements are confirmed by panels (e) and (f) of fig.4, where the effect of increasing the number  $n$  of summed velocities, keeping fixed the value of  $\delta$ , has been investigated. More precisely  $\delta=100$  and  $n = 5000$  in (e) and  $n = 50000$  in (f). As expected, the increment of  $n$  makes the Pdf closer to the Gaussian, essentially because the total time over which the sum is considered increases (for  $n = 50000$  we cover a simulation time of  $5 \times 10^6$ ) and therefore correlations become asymptotically weaker and weaker, thus finally satisfying the prediction of the standard CLT.

In order to study in more details the ensemble-time inequivalence along the QSS regime in the next subsection we will increase the system size and discuss numerical results for  $N = 5000$  and  $N = 50000$ .

*$N=5000$  and  $N=50000$  at  $U=0.69$ .* In fig.5 we show the time evolution of the temperature for the cases  $N = 5000$  and  $N = 50000$  at  $U = 0.69$ , always starting (as usual) from the M1 initial conditions. It is evident that, for both systems, the length of the QSS plateaux is very much greater than for  $N = 100$ .

We discuss first numerical simulations done inside the QSS for  $N = 5000$  and  $U = 0.69$ .



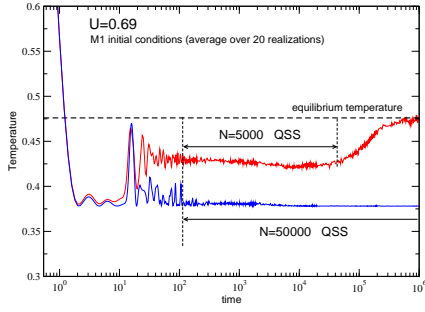


Fig. 5: Temperature time evolution for the HMF system, with  $U = 0.69$ , M1 initial conditions and for  $N = 5000$  and  $N = 50000$ . The presence of a long-lasting QSS regime is clearly visible in both the cases and the plateaux are very much larger then in the  $N = 100$  case.

In fig.6 we show in (a) the ensemble average Pdf of velocities calculated over 1000 realizations at  $t = 100$ , i.e. at the beginning of the QSS regime. Its shape, constant along the entire QSS, is clearly not Gaussian and looks similar to that of fig.3 (a). In panels (b-d) we show the effect of increasing the number  $n$  of velocity terms in the  $y$  sum on the time average Pdfs, calculated using a fixed value of  $\delta = 100$ . An average over 200 different realizations of the initial conditions was also considered in order to have good statistics. In this case only for  $n = 1000$  a  $q$ -Gaussian, with  $q = 1.45 \pm 0.05$ , emerges. This is most likely due not to the effective number of  $n$  used but, consistently with fig.6, to the fact that when choosing a large  $n$  one is averaging over a larger interval of time and thus considers in a more appropriate way the average over the entire QSS regime. In any case the observed behavior goes in the opposite direction to the prescriptions of the standard CLT and to the trend shown in panels (e-f) of fig.4. Indeed, increasing  $n$ , the Pdf tails do not vanish but become more and more evident, thus supporting even further the claim about the existence of a non-Gaussian attractor for the nonergodic QSS regime of the HMF model. Moreover, the results of fig.6 confirm the robustness of the  $q$ -Gaussian shape along the entire QSS plateaux and the inequivalence between ensemble and time averages in the metastable regime.

Let us now definitively demonstrate this inequivalence considering the case  $N=50000$  at  $U=0.69$ . In fig.7 (a) we plot the ensemble average Pdf of the velocities calculated (over 100 different realizations) at  $t = 200$ , i.e. at the beginning of the QSS regime, and after a very long transient, at  $t = 250000$  (full circles). In panel (b) we plot the time average Pdf for the normalized variable  $y$  with  $n = 5000$  and  $\delta = 100$ , after a transient of 200 time units and over a simulation time of 500000 units along the QSS. It is important to stress that in this case *only one single realization* of the initial conditions has been performed, realizing this way a *pure time average*. The shape of the time average Pdf (b) results to be again a robust  $q$ -Gaussian, with

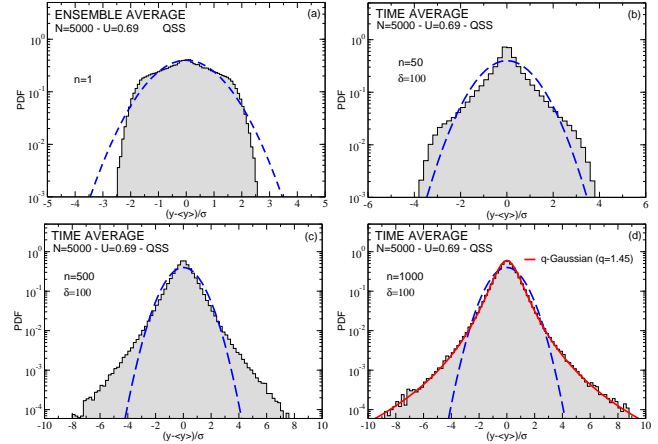


Fig. 6: Numerical simulations for the HMF model with  $N = 5000$ ,  $U = 0.69$  and M1 initial conditions, *in the QSS regime*. (a) Pdf of single rotor velocities at the time  $t = 100$  (ensemble average over 1000 realizations). (b-d) Time average Pdfs for the normalized variable  $y$ , after a transient time of 100 units and considering increasing values of  $n$  with a fixed time interval  $\delta = 100$ , i.e. considering an increasing total simulation time inside the QSS. An average over 200 different realizations of the initial conditions was also considered in order to have a good statistics. Only for  $n = 1000$ , i.e. when the entire QSS extension has been considered (see fig.5), we get a very good  $q$ -Gaussian shape.

$q = 1.4 \pm 0.05$ , not only in the tails, but also in the center (see inset). The time average Pdf is completely different from the ensemble average Pdf of fig.7(a) (that is also very robust over all the plateaux), thus confirming definitively the inequivalence between the two kind of averages and the existence of a  $q$ -Gaussian attractor in the QSS regime of the HMF model. These results indicate that standard statistical mechanics based on the ergodic hypothesis cannot be applied in this case, while a generalized version, like the  $q$ -statistics [1, 2] is likely more suitable [16].

**Conclusions.** — The numerical simulations presented in this paper strongly indicate that dynamical correlations and ergodicity breaking, induced in the HMF model by the initial out-of equilibrium violent relaxation, are present along the entire QSS metastable regime and decay very slowly even after it. In particular, considering finite sums of  $n$  correlated variables (velocities in this case) selected with a constant time interval  $\delta$  along single rotor trajectories, allowed us to study this phenomenon in detail. Indeed, we numerically showed that, in the weakly chaotic QSS regime, (i) ensemble average and time average of velocities are inequivalent, hence the ergodic hypothesis is violated, (ii) the standard CLT is violated, and (iii) robust  $q$ -Gaussian attractors emerge. On the contrary, when no QSS exist, or at a very large time after equilibration, i.e., when the system is fully chaotic and ergodicity has been restored, the ensemble average of velocities results to be equivalent to the time average and one observes a conver-

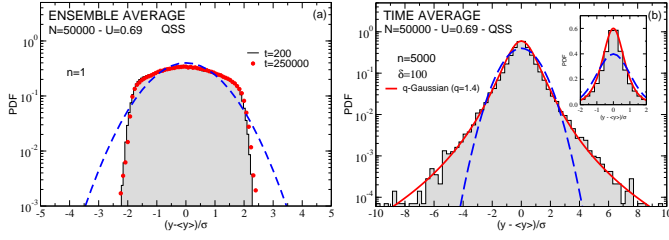


Fig. 7: Numerical simulations for the HMF model for  $N=50000$ ,  $U=0.69$  and M1 initial conditions *in the QSS regime*. (a) Pdfs of single rotor velocities at the times  $t=200$  and  $t=250000$  (ensemble average over 100 realizations). (b) Time average Pdf for the variable  $y$  calculated over *only one single realization* in the QSS regime and after a transient time of 200 units. In this case we used  $\delta = 100$  and  $n = 5000$ , in order to cover a very large portion of the QSS (see fig.5). Again, a  $q$ -Gaussian reproduces very well the calculated Pdf both in the tails and in the central part (see inset). See text for further details.

gence towards the standard Gaussian attractor. In this case, the predictions of CLT are satisfied, even if we have only considered a finite sum of stochastic variables. How fast this happens depends on the size  $N$ , on the number  $n$  of terms summed in the  $y$  variables and on the time interval  $\delta$  considered.

These results are consistent with the recent  $q$ -generalized forms of the CLT discussed in the literature [3–6, 9], and pose severe questions to the often adopted procedure of using ensemble averages instead of time averages. Nonergodicity in coupled many particle systems goes back to the famous FPU experiment [26], but in our case is due to the long-range nature of the interaction. More recently, nonergodicity was found in deterministic iterative systems exhibiting subdiffusion [11], but also in real experiments of shear flows, with results that were fitted with Lorentzians, i.e.,  $q$ -Gaussians with  $q = 2$  [23]. The whole scenario reminds that found for the leptokurtic *returns* Pdf in financial markets [24], or in turbulence [25], among many other systems, and could probably explain why  $q$ -Gaussians appear to be ubiquitous in complex systems. Finally, we would like to add that, although it is certainly nontrivial to prove analytically whether the attractor in the nonergodic QSS regime of the HMF model precisely is a  $q$ -Gaussian or not (analytical results, as well as numerical dangers, have been recently illustrated in ref. [8] for various models), our numerical simulations unambiguously provide a very strong indication towards the existence of a robust  $q$ -Gaussian attractor in the case considered. This opens new ways to the possible application of the  $q$ -generalized statistics in long-range Hamiltonian systems which will be explored in future papers.

\*\*\*

We thank Marcello Iacono Manno for many technical discussions and help in the preparation of the scripts to

run our codes on the GRID platform. The numerical calculations here presented were done within the TRIGRID project. A.P. and A.R. acknowledge financial support from the PRIN05-MIUR project "Dynamics and Thermodynamics of Systems with Long-Range Interactions". C.T. acknowledges financial support from the Brazilian Agencies Pronex/MCT, CNPq and Faperj.

## REFERENCES

- [1] TSALLIS C., *J. Stat. Phys.*, **52** (1988) 479
- [2] TSALLIS C., GELL-MANN M. and SATO Y., *Europhys. News*, **36** (2006) 186, and references therein
- [3] TSALLIS C., *Milan J. Mathematics*, **73** (2005) 145, and references therein
- [4] S. UMAROV, C. TSALLIS AND S. STEINBERG, *cond-mat/0603593*, (2006)
- [5] TIRNAKLI U., BECK C. and TSALLIS C., *Phys. Rev. E*, **75** (2007) 040106 (R)
- [6] TSALLIS C., RAPISARDA A., PLUCHINO A. and BORGES E.P., *Physica A*, **341** (2007) 143
- [7] F. BALDOVIN F. and A. STELLA, *Phys. Rev. E*, **75** (2007) 020101(R)
- [8] HILHORST H.J. and SCHEHR G., *Jstat*, **06** (2007) P06003
- [9] VIGNAT C. and PLASTINO A., *arXiv:0706.0151[cond-mat.stat-mech]*, (2007)
- [10] THISTLETON W.J., MARSH J.A., NELSON K. and TSALLIS C., *IEEE, in press, cond-mat/0605570*, (2006)
- [11] BEL G. and BARKAI E., *Europhys. Lett.*, **74** (2006) 15
- [12] DAUXOIS T., LATORA V., RAPISARDA A., RUFFO S. and TORCINI A., *Lecture Notes in Physics*, edited by T. DAUXOIS, S. RUFFO, E. ARIMONDO, M. WILKENS, Vol. **602** 2002, p. 458
- [13] LATORA V., RAPISARDA A. and RUFFO S., *Phys. Rev. Lett.*, **80** (1998) 692
- [14] LATORA V., RAPISARDA A. and TSALLIS C., *Phys. Rev. E*, **64** (2001) 056134
- [15] PLUCHINO A., LATORA V. and RAPISARDA A., *Physica D*, **193** (2004) 315
- [16] RAPISARDA A. and PLUCHINO A., *Europhysics News*, **36** (2005) 202
- [17] PLUCHINO A., LATORA V. and RAPISARDA A., *Physica A*, **370** (2006) 573
- [18] GIANISANTI A., MORONI D. and CAMPA A., *Physica A*, **305** (2002) 137
- [19] CHAVANIS P.-H., *Eur. J. Phys. B*, **53** (2006) 487
- [20] ANTONIAZZI A., CALIFANO F., FANELLI D., and RUFFO S., *Phys. Rev. Lett.*, **98** (2007) 150202
- [21] MORITA H. and KANEKO K., *Phys. Rev. Lett.*, **96** (2006) 050602
- [22] TAMARIT F., MAGLIONE G., STARIOLO D. A., and ANTENEOD C., *Phys. Rev. E*, **71** (2005) 036148
- [23] WANG Y., KRISHAN K. and DENNIN M., *Phys. Rev. Lett.*, **98** (2007) 220602
- [24] MANTEGNA A. and STANLEY H.E., *An Introduction to Econophysics*, edited by CAMBRIDGE UNIVERSITY PRESS, CAMBRIDGE 1999
- [25] BECK C., LEWIS G.S. and SWINNEY H.L., *Phys. Rev. E*, **63** (2001) 035303
- [26] FOR AN UPDATED DISCUSSION OF THE FPU PROBLEM SEE THE SPECIAL ISSUE, *Chaos*, **15** (2005)